PALEOCEANOGRAPHY, VOL. 6, NO. 2, PAGES 275-290, APRIL 1991

EVOLUTION OF MODERN DEEPWATER CIRCULATION: EVIDENCE FROM THE LATE MIOCENE SOUTHERN OCEAN

James D. Wright[1]

Lamont-Doherty Geological Observatory of Columbia University, Palisades, New York

Kenneth G. Miller[2]

Department of Geological Sciences, Rutgers University, New Brunswick, New Jersey

Richard G. Fairbanks

Lamont-Doherty Geological Observatory of Columbia University, Palisades, New York

Abstract. Deepwater circulation plays an important role in climate modulation through its redistribution of heat and salt and its control of atmospheric CO_2. Oppo and Fairbanks (1987) showed that the Southern Ocean is an excellent monitor of deepwater circulation changes for two reasons: (1) the Southern Ocean is a mixing reservoir for incoming North Atlantic Deep Water and recirculated water from the Pacific and Indian oceans; and (2) the nutrient/$\delta^{13}C$ tracers of deepwater are not significantly changed by surficial processes within the Southern Ocean. We can extend these principles to the late Miocene because tectonic changes in the Oligocene and early and middle Miocene developed near-modern basinal configurations. However, on these time scales, changes in the oceanic carbon reservoir and mean ocean nutrient levels also affect the $\delta^{13}C$ differences between ocean basins. From 9.8 to 9.3 Ma, Southern Ocean $\delta^{13}C$ values oscillated between high North Atlantic values and low Pacific values. The Southern Ocean recorded $\delta^{13}C$ values similar to Pacific values from 9.2 to 8.9 Ma, reflecting a low contribution of Northern Component Water (NCW). The $\delta^{13}C$ differences between the NCW and Pacific Outflow Water (POW) end-members were low from 8.9 to 8.0 Ma, making it difficult to discern circulation patterns. NCW production may have completely shutdown at 8.6 Ma, allowing Southern Component Water (SCW) to fill the North Atlantic and causing the $\delta^{13}C$ values in the North Atlantic, Pacific, and Southern oceans to converge. Deepwater $\delta^{13}C$ patterns resembling the modern distributions evolved by 7.0 Ma: $\delta^{13}C$ values were near 1.0 ‰ in the North Atlantic; 0.0 ‰ in the Pacific; and 0.5 ‰ in the Southern Ocean. Development of near-modern $\delta^{13}C$ distributions by 7.0 Ma resulted not only from an increase in NCW flux but also from an increase in deepwater nutrient levels. Both of these processes increased the $\delta^{13}C$ difference between the North Atlantic and Pacific oceans. Deepwater circulation patterns similar to today's operated as early as 9.8 Ma, but were masked by the lower nutrient/$\delta^{13}C$ differences. During the late Miocene, "interglacial" intervals prevailed during intervals of NCW production, while "glacial" intervals occurred during low NCW production.

INTRODUCTION

Deep ocean circulation is driven by density differences. At present, relatively warm, high-salinity water sinks in the Norwegian-Greenland Sea and northern North Atlantic, while circum-Antarctic cooling produces a colder, lower salinity deep water mass. In both cases, deepwater production is linked to surface water density, reflecting preconditioning by the processes of low-latitude evaporation, high-latitude cooling, or freezing. These processes controlled the past production of deep and intermediate water masses.

The locations and rates of deepwater production are crucial to the modulation of climate. For example, the production of North Atlantic Deep Water (NADW) releases heat to the North Atlantic north of 35°N which is equivalent to 25% of incoming solar radiation [Broecker and Denton, 1989]. In

[1]Also at Department of Geological Sciences, Columbia University, New York.
[2]Also at Lamont-Doherty Geological Observatory, Palisades, New York.

Paper number 90PA02498.
0883-8305/91/90PA-02498 $10.00

addition, atmospheric CO_2 concentrations in the late Pleistocene varied between glacial values of 180 ppm and interglacial values of 280 ppm [Delmas et al., 1980; Neftel et al., 1982; Stauffer et al., 1985]. These changes are also thought to be associated with varied production of NADW and changes in intermediate water source areas, because the ocean is the largest reservoir of CO_2 (~60 times larger than the atmosphere) [e.g., Siegenthaler et al., 1980; Broecker, 1982; Oeschger et al., 1983; Boyle, 1989; Oppo et al., 1990]. Accordingly, pre-Pleistocene deepwater circulation patterns may have been linked to climate changes.

Deep water masses are distinguished in today's ocean by temperature, salinity, density, and geochemical tracers (e.g., silica, phosphate, oxygen, nitrate). However, reconstructions of past oceans rely primarily on $\delta^{13}C$ distributions because this tracer is readily measured in sediments. The nutrient content of NADW is low and its $\delta^{13}C$ value is high [Kroopnick, 1985] because NADW is composed largely of upper ocean water [Worthington, 1970]. In contrast, only a small portion of surface water composes Antarctic Bottom Water (AABW) [Mantyla and Reid, 1983], and as a result, AABW has a higher nutrient content and a lower $\delta^{13}C$ value. These nutrient and $\delta^{13}C$ characteristics distinguish AABW from NADW.

Late Pleistocene deepwater circulation patterns have been identified using benthic foraminiferal $\delta^{13}C$ distributions [e.g., Shackleton et al., 1983; Boyle and Keigwin, 1982, 1987; Curry and Lohmann, 1982; Oppo and Fairbanks, 1987; Duplessy et al., 1988; Oppo et al., 1990]. Paleoceanographers have used these Pleistocene strategies to estimate deepwater circulation patterns for the late Pliocene to Paleocene [e.g., Miller and Fairbanks, 1985; Raymo et al., 1989; Woodruff and Savin, 1989].

Most studies agree that Northern Component Water (NCW, analogous to NADW) production began prior to the late Miocene [Schnitker, 1980; Blanc and Duplessy, 1982; Miller and Fairbanks, 1985; Woodruff and Savin, 1989]. It was during the late Miocene that modern $\delta^{13}C$ differences were established between the deep Atlantic and Pacific oceans [e.g., Bender and Keigwin, 1979; Miller and Fairbanks, 1985; Woodruff and Savin, 1989]. However, Atlantic and Pacific differences in $\delta^{13}C$ values alone cannot be used to quantify NCW fluxes [Oppo and Fairbanks, 1987]. We can estimate the changes in NCW flux with the $\delta^{13}C$ record from the Southern Ocean [Oppo and Fairbanks, 1987] and evaluate the role of deepwater circulation in the evolution of modern $\delta^{13}C$ patterns during the late Miocene.

THE SOUTHERN OCEAN APPROACH

The Southern Ocean plays an important role in the distribution of nutrients and $\delta^{13}C$ values. It receives NADW and mixes it with recirculated Pacific and Indian Outflow Water (POW and IOW). AABW and Antarctic Intermediate Water (AAIW) are derived from Southern Ocean water and spread to the north. The influences of NADW, IOW, and POW on the Southern Ocean are distinguishable from sector to sector only by minor variations in water mass characteristics (e.g., potential temperature, salinity, and silica content) [Georgi, 1981; Mantyla and Reid, 1983]. The generally uniform $\delta^{13}C$ values in the deep Southern Ocean or Circumpolar Deep Water (CPDW) indicate that it is relatively well mixed with respect to this tracer [Kroopnick, 1985]. The nutrient or $\delta^{13}C$ compositions in CPDW are not significantly modified through surface processes (i.e., air-sea interaction and/or biological processes) because there is little surface water in this water mass [Mantyla and Reid, 1983]. As a result, CPDW $\delta^{13}C$ values plot on a mixing line between the NADW and POW end-members and are indicative of the relative contribution from each ocean.

Oppo and Fairbanks [1987] first used the deep Southern Ocean as a monitor of glacial/interglacial changes in the NCW flux. By comparing Pleistocene $\delta^{13}C$ records from the North Atlantic, Pacific, and Southern oceans, they not only documented that the NCW flux during the last glacial maximum was low as previously inferred [Boyle and Keigwin, 1982; 1987; Curry and Lohmann, 1982; Shackleton et al., 1983], but also quantified its relative contribution to the Southern Ocean. Oppo and Fairbanks [1987] mapped the $\delta^{13}C$ of bottom water in contact with the seafloor and noted a sharp mixing zone boundary between NADW and AABW. Small changes in the location of this mixing zone can result in different regional distribution of measured $\delta^{13}C$ signals. In addition, Oppo and Fairbanks [1987] illustrated that it is not possible to determine the flux of NADW by monitoring sites only in the North Atlantic and Pacific.

The Southern Ocean approach of Oppo and Fairbanks [1987] is applicable to the late Miocene ocean because near-modern basinal configurations were established prior to the late Miocene. During the Oligocene, the Drake Passage opened and Tasman Plateau deepened, removing the physical barriers to circumpolar flow [Barker and Burrell, 1977; Weissel et al., 1977]. Other tectonic changes that occurred during the early and middle Miocene include the closure of the eastern Paratethys by the late early Miocene [Berggren and Van Couvering, 1974; Rogl and Steininger, 1984], the restriction of surface water flow through the Indo-Pacific Passage by the end of the middle Miocene [Hamilton, 1979], and intermittent movement along Atlantic fracture zones and tectonically active ridges during the early and middle Miocene [Luyendyk et al., 1979; Miller and Tucholke, 1983]. The subsidence history of the Greenland-Scotland Ridge is controversial, and surface water connections may have existed across this gateway during the Eocene to Oligocene [Miller and Tucholke, 1983]. However, various studies agree that the Iceland-Faroe section of the ridge subsided sufficiently by the middle Miocene to allow an equivalent of Norwegian Sea Water to overflow into the North Atlantic [e.g., Schnitker, 1980; Theide and Eldholm, 1983; Miller and Tucholke, 1983].

SETTING AND CORE SELECTION

The residence time of deepwater within the modern Atlantic Ocean is short; therefore, $\delta^{13}C$ distributions in the Atlantic primarily represent mixing between southward flowing NADW (high salinity, high $\delta^{13}C$ values) and northward flowing AABW and AAIW (lower salinity, lower $\delta^{13}C$ values) (Figure 1) [Broecker, 1979]. North Atlantic Deep Water is the dominant water mass in the North Atlantic, although the influence of AABW is present as far as 40°N at depths greater than 4500 m (Figure 1).

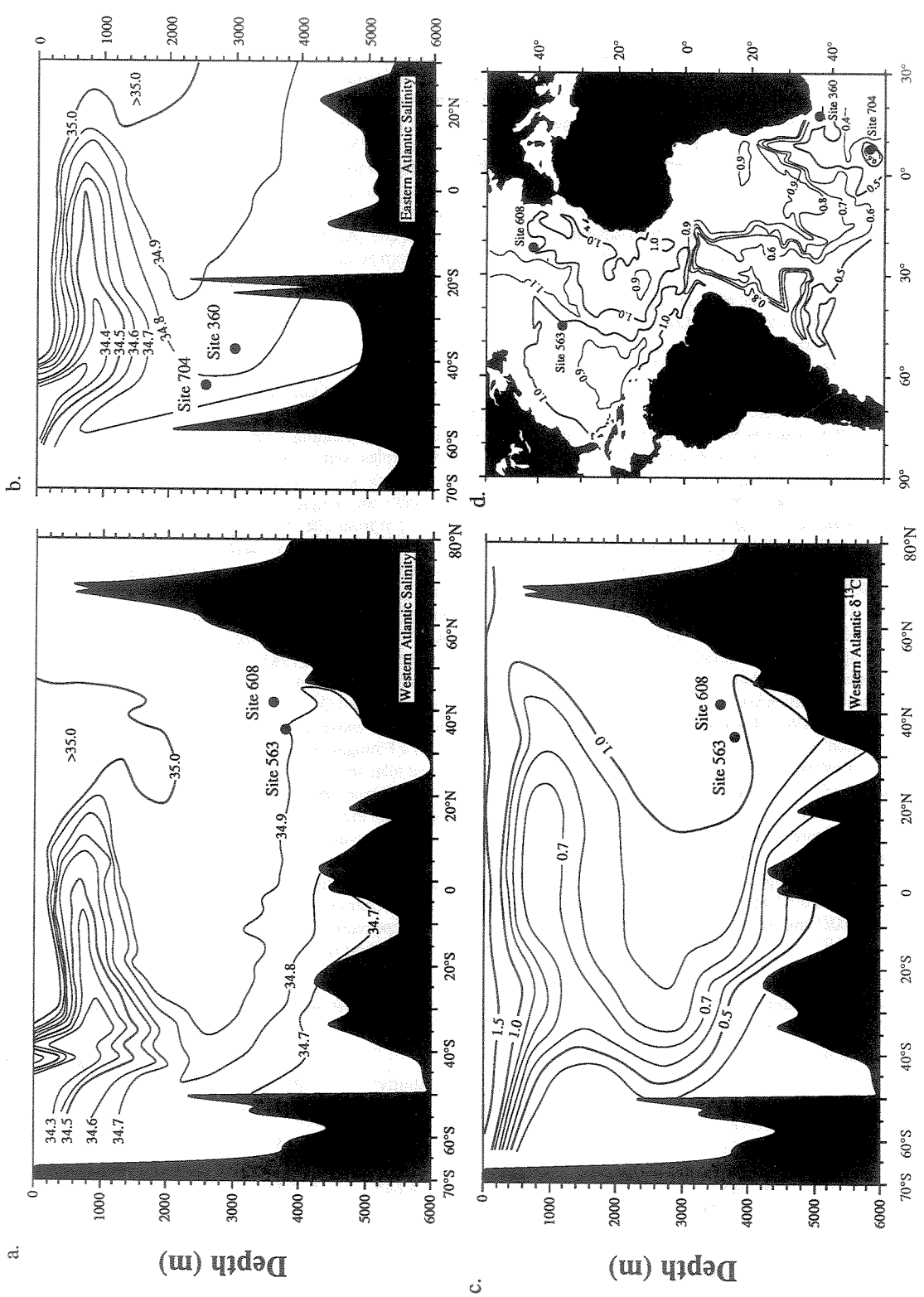

Fig. 1. Site locations with respect to salinity in western Atlantic and eastern Atlantic GEOSECS transects (Figures 1a and 1b); $\delta^{13}C$ in the western Atlantic GEOSECS transect (Figure 1c, after Kroopnick [1985]); and predicted $\delta^{13}C$ at the sediment-water interface (Figure 1d, from Oppo and Fairbanks [1987]).

Deep Sea Drilling Project (DSDP) Sites 563 and 608 were used to represent the NCW end-member in the late Miocene. Site 563 was drilled on the western flank of the Mid-Atlantic Ridge [Bougault et al., 1985], while Site 608 was drilled in the eastern basin on the southern flank of the King's Trough Complex (Table 1 and Figure 1d) [Ruddiman et al., 1987]. Hole 563 only recovered sediments older than ~8 Ma; we used the isotope record from Site 608 to represent the NCW end-member from the interval 8.0 to 5.3 Ma. Both Sites 563 and 608 are south of the region of NCW formation and may be subject to mixing with Southern Component Water (SCW, as defined by Broecker and Peng [1982]). There are no suitable cores closer to the region of NCW formation. However, Sites 563 and 608 are well situated to represent NCW $\delta^{13}C$ values. Advantages afforded by Sites 563 and 608 are that they appear to lack major unconformities in the upper Miocene sections and have reliable magnetostratigraphy [Miller et al., 1985, 1991a; Clement and Robinson, 1986]. Sites 563 and 608 would fail to represent the NCW end-member only during a drastic decrease in NCW production.

In today's ocean, bottom water at Site 563 is composed of 87% NCW and 13% SCW, while Site 608 is bathed by 91% NCW and 9% SCW (Table 1 and Figure 1). The $\delta^{13}C$ value of bottom water at Sites 563 and 608 is near 1.0 ‰ (Figure 1d). The small difference in the percentage of NCW at these sites is a function of latitude and depth (Table 1). At present, Site 563 is ~5°S of and 260 m deeper than Site 608, and, therefore, it is more influenced by SCW.

Sites 360 and 704 were selected to monitor the NCW contribution to the Southern Ocean (Figure 1b). Both sites offer nearly complete upper Miocene sections with relatively high sedimentation rates (30 to 40 m/m.y.). The most intense gradients in water mass properties are in the South Atlantic where NADW separates AABW and AAIW (Figure 1). Located within this region, Sites 360 and 704 should record variations in the flux of NCW. DSDP Site 360 was drilled in the Cape Basin [Bolli et al., 1978]. Water-mass properties suggest that this site is currently bathed by a mixture of 55% NCW and 45% CPDW (Figure 1 and Table 1). Ocean Drilling Program Site 704 was drilled on the Meteor Rise [Ciesielski et al., 1988] with a water-mass composition of 35% NCW and 65% CPDW. The predicted $\delta^{13}C$ values for the bottom water at Sites 360 and 704 are 0.7 and 0.6 ‰, respectively (Figure 1d).

In today's ocean, POW has a $\delta^{13}C$ value of 0.0 ‰. This value represents the mixing between SCW (0.4 ‰) and North Pacific water (-0.5 ‰) [Kroopnick, 1985]. SCW ages as it flows northward in the deepest Pacific, resulting in low $\delta^{13}C$ values in the North Pacific [Kroopnick, 1985]. Deepwater from the Pacific returns to the Southern Ocean as recirculated POW, which is an intermediate and upper deep water mass. Changes in the $\delta^{13}C$ value of POW largely reflect changes in the mean deep water value; deepwater circulation patterns can only effect minor changes in the Pacific composition because it is such a large reservoir. For the late Miocene, Ontong Java Plateau Site 289 [Andrews et al., 1975] ideally represents POW (western equatorial Pacific) [Savin et al., 1981, 1985; Woodruff et al., 1981; Woodruff and Savin, 1989].

METHODS

Approximately one sample per meter was obtained from the upper Miocene section at Site 563 [this study; Miller and Fairbanks, 1985], yielding a sample resolution of 50 kyr. At Site 608, samples were taken every 2 m, yielding a sample resolution of 100 kyr. For the Southern Ocean sites, approximately one sample per 3 m from Site 360 and 1 sample per 2 m from Site 704 were studied, yielding average sample resolutions of 100 kyr. and 50 kyr., respectively. This resolution should permit recognition of first-order (10^6 year) circulation patterns. *Cibicidoides* spp. and *Planulina wuellerstorfi* were picked from the greater than 250-μm fraction. These taxa accurately record $\delta^{13}C$ variations in seawater [Belanger et al., 1981; Graham et al., 1981]. Their $\delta^{18}O$ values are lower than equilibrium values by about 0.64‰ [e.g., Shackleton and Opdyke, 1973]. Samples were analyzed by a Carousel-48 automatic carbonate preparation device attached to a Finnigan MAT 251 mass spectrometer. Results are reported relative to the PDB standard (Table 2).

Backtracked paleodepths were estimated for each site by assuming simple thermal subsidence and using the empirical age-subsidence curves after Sclater et al. [1971] and Berger and Winterer [1974]. We computed late Miocene paleodepths for each site using the equations of Miller et al. [1989] (Table 1).

A uniform scheme for age assignments is essential to correlate isotope records from different ocean basins. The most unequivocal method is to correlate to the Geomagnetic Polarity

TABLE 1. Location and Water Mass Properties of Present-Day End-Members and DSDP and ODP Sites Discussed in the Text

End-Member Site	Latitude	Longitude	Present Depth (m)	Paleo-depth (m)	Salinity (‰)	Potential Temperature (°C)	Percent NCW vs SOW	Percent NCW vs POW
NCW					34.94*	2.5*		
CPDW					34.71*	0.62*		
POW					34.67*	1.5*		
289	00°30'S	158°31'E	2206	2300	34.66	1.74	-	0%
360	35°51'S	18°05'E	2949	3000	34.84	2.11	56%	70%
563	37°46'N	43°46'W	3786	3600	34.91	2.13	87%	100%
608	42°50'N	23°05'W	3526	3500	34.92	2.25	91%	100%
704	46°53'S	7°25'E	2531	2450	34.79	2.05	35%	60%

*Values defined by Broecker and Peng [1982].

TABLE 2. Upper Miocene $\delta^{18}O$ and $\delta^{13}C$ Data From Sites 360, 563, 608, and 704B

Sample	Depth	Age	$\delta^{18}O$	$\delta^{13}C$
		Site 360		
4-1 13-17	109.25	5.33	2.22	0.43
4-3 15-19	112.10	5.40	2.30	0.86
5-1 105-109	118.55	5.55	2.56	0.52
5-3 90-94	121.40	5.62	2.54	0.38
5-5 101-105	124.50	5.69	2.53	0.40
6-1 104-108	128.54	5.78	2.58	0.40
6-3 109-113	131.59	5.86	2.47	0.44
6-5 105-109	134.55	5.93	2.45	0.17
6-5 105-109	134.55	5.93	2.39	0.06
7-1 124-128	137.74	6.00	2.46	-0.38
7-1 124-128	137.74	6.00	2.47	-0.34
7-3 123-127	140.73	6.11	2.65	0.35
7-5 102-106	143.52	6.22	2.42	0.25
8-1 102-106	147.02	6.35	2.55	0.17
8-3 90-94	149.60	6.45	2.53	0.21
9-1 104-108	156.54	6.71	2.58	0.29
9-3 92-96	159.42	6.82	2.48	0.31
9-5 101-105	162.51	6.94	2.37	0.58
10-1 110-114	166.10	7.08	2.36	0.59
10-3 100-104	169.00	7.19	2.37	0.59
10-3 135-139	169.35	7.20	2.19	0.78
11-3 20-24	177.70	7.52	2.02	0.83
11-3 106-110	178.56	7.55	2.26	0.89
11-5 102-106	181.52	7.66	2.19	0.78
12-1 122-126	185.22	7.80	2.22	0.84
12-2 110-114	186.60	7.85	2.30	0.84
12-3 104-108	188.04	7.91	2.35	0.69
12-5 106-110	191.06	8.02	2.28	0.91
13-1 90-94	194.40	8.15	2.43	1.05
13-2 70-74	195.70	8.20	2.32	0.97
13-3 90-94	197.40	8.26	2.42	0.82
13-4 101-105	199.01	8.33	2.07	1.02
13-5 90-94	200.40	8.38	2.36	1.13
13-5 90-94	200.40	8.38	2.38	1.07
13-6 130-136	202.30	8.45	2.37	1.37
14-2 110-114	205.50	8.57	2.21	1.18
14-2 110-114	205.50	8.57	2.12	1.04
14-3 90-94	206.90	8.62	2.17	0.94
14-4 90-94	207.40	8.63	2.34	0.97
14-5 102-106	209.02	8.69	2.30	0.69
14-5 140-144	210.40	8.76	2.14	0.82
15-1 89-93	213.39	8.91	2.23	0.83
15-2 111-115	215.11	9.40	2.24	0.75
16-1 140-144	223.40	9.42	1.93	1.01
16-2 40-44	223.90	9.44	1.88	0.96
16-2 130-134	224.80	9.51	2.07	0.73
16-3 19-23	225.19	9.51	2.13	1.09
16-3 120-124	226.20	9.55	2.07	1.05
16-4 30-34	226.80	9.57	1.89	1.10
16-4 30-34	226.80	9.57	1.86	1.00
16-4 109-113	227.59	9.60	2.07	0.99
17-1 108-112	232.58	9.81	2.12	1.03
17-1 108-112	232.58	9.81	2.10	0.70
17-2 47-51	233.47	9.84	2.05	0.91
17-2 130-134	234.30	9.88	1.89	0.95
17-3 40-44	234.90	9.91	1.95	0.85
17-3 123-127	235.73	9.95	1.79	0.68
18-1 40-44	241.40	10.25	2.01	0.86
18-1 105-109	242.05	10.28	2.04	0.66
18-2 90-94	243.40	10.35	2.17	0.74
		Site 563		
1-1 43-47	161.43	8.40	1.98	1.11
1-2 19-23	162.69	8.45	2.11	1.45
1-2 94-98	163.44	8.48	2.12	1.42
1-3 69-73	164.69	8.53	1.79	1.19
2-1 120-124	167.20	8.62	1.82	1.15
2-2 30-34	167.80	8.65	2.09	0.81
2-2 30-34	167.80	8.65	2.03	0.84
2-2 110-114	168.60	8.68	1.96	0.84
2-3 31-35	169.31	8.70	1.98	1.03
2-3 40-44	169.40	8.71	1.88	1.06
2-3 111-115	170.11	8.73	1.97	1.04
2-4 112-115	171.62	8.79	1.82	1.12
2-5 19-23	172.19	8.81	2.02	1.01
2-5 38-42	172.38	8.82	1.95	1.14
2-5 108-112	173.08	8.85	1.81	1.12
2-6 30-34	173.80	8.87	1.94	0.96
2-6 40-44	173.90	8.88	2.11	1.10
2-6 110-114	174.60	8.90	1.86	1.03
2-7 31-35	175.31	8.96	1.93	1.06
3-1 119-123	176.69	9.11	2.05	0.96
3-2 35-39	177.35	9.19	1.86	1.22
3-2 116-120	178.16	9.28	2.08	1.18
3-2 140-144	178.40	9.31	2.02	1.31
3-3 31-35	178.81	9.36	1.76	1.22
3-3 111-115	179.61	9.45	1.67	1.34
3-3 138-142	179.88	9.48	2.01	1.28
3-4 111-115	181.11	9.63	2.28	1.23
3-5 38-42	181.88	9.71	2.11	1.01
3-5 111-115	182.61	9.80	1.44	1.18
3-5 136-140	182.86	9.83	1.93	1.14
3-6 31-35	183.31	9.88	1.64	1.10
3-6 110-114	184.10	9.97	1.65	1.03
3-6 120-124	184.20	9.98	1.90	1.37
4-1 116-120	186.16	10.21	1.94	0.99
4-2 31-35	186.81	10.28	1.74	0.90
4-2 100-104	187.50	10.36	1.85	0.93
4-2 110-114	187.60	10.37	1.70	1.03
4-3 34-38	188.34	10.44	1.912	0.91
4-3 135-139	189.35	10.52	2.15	1.05
		Site 608		
16-1 62-66	142.02	5.58	2.23	1.04
16-3 75-79	145.15	5.73	2.21	0.81
16-4 90-94	146.80	5.82	2.25	0.66
16-5 71-75	148.11	5.88	2.25	0.69

TABLE 2. (continued)

Sample	Depth	Age	$\delta^{18}O$	$\delta^{13}C$
	Site 608 (continued)			
16-7 19-23	150.59	6.00	2.27	0.86
17-1 64-68	151.64	6.05	2.32	0.69
17-2 59-63	153.09	6.12	2.37	0.79
17-3 101-105	155.01	6.22	2.30	0.63
18-1 100-104	157.50	6.34	2.17	1.07
18-3 70-74	160.20	6.47	2.14	0.93
18-3 89-93	163.39	6.63	2.15	1.15
19-1 70-74	166.80	6.80	2.03	1.07
19-2 66-70	168.26	6.87	1.97	1.06
19-3 73-77	169.83	6.94	2.09	1.34
19-5 75-79	172.85	7.09	2.01	1.23
20-1 126-130	176.96	7.29	1.91	0.97
20-3 119-123	179.89	7.44	2.10	1.13
20-5 119-123	182.89	7.59	2.07	1.04
21-1 70-74	186.00	7.75	2.07	1.37
21-2 100-104	187.80	7.85	2.21	1.27
21-3 79-83	189.09	7.91	2.04	1.14
21-4 49-53	190.29	7.96	2.12	1.48
21-5 80-84	192.10	8.04	2.06	1.67
22-2 86-90	197.26	8.27	2.10	1.14
22-4 80-84	200.20	8.40	2.16	1.04
23-1 57-61	205.07	8.62	1.98	1.06
23-4 88-92	209.88	8.83	1.77	0.78
23-5 80-84	211.30	8.89	1.99	1.01
23-7 40-44	213.90	9.02	1.96	1.19
24-1 18-22	214.28	9.04	2.12	1.13
24-3 74-78	217.84	9.22	2.03	1.20
24-4 73-77	219.33	9.30	1.99	1.16
24-5 82-86	220.92	9.38	2.11	1.17
24-6 47-51	222.07	9.44	2.07	1.30
24-7 4-8	223.14	9.49	2.06	1.26
25-1 99-103	223.99	9.54	2.20	1.12
25-2 33-37	225.55	9.64	2.00	1.16
25-3 68-72	227.38	9.71	2.17	0.96
25-5 92-96	230.62	9.87	2.10	0.79
25-6 107-111	232.27	9.96	1.90	0.91
25-7 14-18	232.84	9.98	1.81	1.06
26-1 78-82	234.08	10.05	2.02	0.85
26-2 30-34	235.10	10.10	2.12	0.92
26-4 27-31	238.07	10.25	2.08	0.79
27-1 3-7	242.93	10.50	2.06	0.66
	Site 704B			
28-2 8-11	253.28	6.40	2.47	1.32
28-4 8-11	256.28	6.54	2.83	1.31
28-6 8-11	259.28	6.69	2.65	1.20
29-1 68-72	261.88	6.80	2.59	1.01
29-2 68-72	263.38	6.87	2.71	1.23
29-3 68-72	264.88	6.93	2.43	0.85
29-4 68-72	266.38	7.00	2.75	1.01
29-5 68-72	267.88	7.07	2.53	1.15
29-6 68-72	269.38	7.13	2.79	1.25
29-7 68-72	269.38	7.13	2.65	1.23
29cc	270.50	7.18	2.23	1.45

TABLE 2. (continued)

Sample	Depth	Age	$\delta^{18}O$	$\delta^{13}C$
	Site 704B (continued)			
30-1 30-34	271.00	7.20	2.47	1.26
30-2 30-34	272.50	7.27	2.77	0.96
30-5 30-34	274.00	7.33	2.65	1.20
30-4 30-34	275.50	7.40	2.70	1.33
30-5 30-34	277.00	7.45	2.61	1.08
30-6 30-34	278.70	7.51	2.28	1.05
30-7 30-34	280.00	7.55	2.68	0.96
30cc	280.10	7.57	2.42	1.28
31-1 33-37	280.53	7.59	2.64	1.26
31-2 33-37	282.03	7.62	2.44	1.03
31-4 33-37	285.03	7.72	2.32	1.15
31-6 33-37	288.03	7.83	2.42	1.04
32-2 10-14	291.30	7.92	2.60	1.32
32-2 10-14	291.30	7.92	2.73	1.41
32-4 10-14	294.30	7.99	2.19	0.97
32-4 10-14	294.30	7.99	2.16	0.91
32-6 10-14	296.30	8.03	2.51	1.22
32cc	299.10	8.10	2.50	0.94
33-2 30-34	301.00	8.14	2.56	1.48
33-4 30-34	304.00	8.20	2.29	1.01
33-6 30-34	307.00	8.27	2.40	0.96
34-2 30-34	310.50	8.35	1.99	1.29
34-4 30-34	313.50	8.41	2.50	1.35
34-6 30-34	316.50	8.48	2.41	1.33
35-2 32-36	320.02	8.55	2.33	0.83
35-4 32-36	323.02	8.61	2.32	0.92
35-5 32-36	324.52	8.64	2.60	1.11
35-6 32-36	326.02	8.67	2.35	0.89
35-7 32-36	327.52	8.70	2.38	0.99
35cc	327.70	8.70	2.14	0.76
36-1 14-18	327.84	8.71	2.15	0.94
36-2 14-18	329.34	8.74	2.65	0.83
36-3 14-18	330.84	8.77	2.23	0.93
36cc	331.65	8.78	2.39	0.95
37-1 25-29	337.45	8.90	2.20	0.90
37-2 25-29	338.95	8.93	2.20	0.89
37-3 25-29	340.45	8.96	1.96	0.57
37-3 25-29	340.45	8.96	2.12	0.64
37cc	346.45	9.05	2.28	0.79
38cc	346.90	9.10	2.14	0.71
39-1 25-29	356.45	9.30	2.35	0.57
39-2 25-29	357.95	9.33	2.09	1.21
39-3 25-29	359.45	9.36	2.32	1.11
39-4 25-29	360.95	9.39	2.25	1.00
39-5 25-29	362.45	9.42	2.31	0.64
39-6 25-29	363.95	9.46	2.21	0.74
39-7 25-29	365.45	9.49	2.15	1.18
39cc	365.65	9.49	2.27	0.88
40-1 68-72	366.38	9.51	2.16	1.06
40-2 68-72	367.88	9.54	2.30	1.05
40-2 68-72	367.88	9.54	2.43	1.03
40-3 68-72	369.38	9.57	2.48	0.84
40-4 68-72	370.88	9.60	2.53	0.69
40-5 68-72	372.38	9.63	2.58	0.90
40-6 68-72	373.88	9.67	2.34	0.55

TABLE 2. (continued)

Sample	Depth	Age	$\delta^{18}O$	$\delta^{13}C$
	Site 704 B (continued)			
40cc	375.10	9.69	2.35	1.10
41-1 60-64	375.80	9.72	2.33	1.04
41-2 60-64	377.30	9.75	2.16	0.87
41-3 60-64	378.80	9.77	2.55	1.04
41-4 60-64	380.30	9.80	2.26	1.13
41-5 60-64	381.80	9.83	2.18	1.00
41-6 60-64	383.30	9.86	2.37	1.13
41cc	384.50	9.89	2.16	0.88
42-2 114-118	387.34	9.95	1.93	0.86
42-5 34-38	391.04	10.03	2.13	0.85
43-2 38-42	396.08	10.13	2.17	0.99
43-6 38-42	401.08	10.24	2.14	1.07
44-1 123-127	404.93	10.32	2.09	0.95
44cc	405.70	10.34	2.14	0.87
45-1 51-55	413.51	10.50	2.33	0.61
45-2 51-55	415.01	10.53	2.10	1.08
45cc	416.40	10.56	2.13	1.16
46-1 135-139	425.55	10.75	2.25	0.89
46-3 135-139	427.05	10.79	2.14	0.43
46-3 135-139	427.05	10.79	2.18	0.70

Time Scale (GPTS). Magnetostratigraphy is available for Sites 563 [Miller et al., 1985], 608 [Clement and Robinson, 1986; Miller et al., 1991a], and 704 [Hailwood and Clement, 1990], while Sites 289 and 360 have no paleomagnetic data. We correlated the latter sites with Sites 563 and 608 and the GPTS by first using published biostratigraphy [Srinivasan and Kennett, 1981; Jenkins, 1978], ongoing biostratigraphic studies of Site 360 (J. Wright, manuscript in preparation), and the magneto-biostratigraphic ages of Berggren et al. [1985]. However, biostratigraphic uncertainties often limit the ability to provide accurate age assignments [Miller and Kent, 1987]. Once moved into a basic stratigraphic framework, $\delta^{18}O$ changes were used to correlate records since global $\delta^{18}O$ variations recorded in the benthic foraminiferal calcite provide distinct tie points for cores in different oceans [e.g., see Miller et al., 1991b; Wright and Miller, 1991]. Age estimates based on $\delta^{18}O$ correlations are consistent with age estimates from biostratigraphic first and last occurrences. Carbon isotope comparisons are sensitive to minor correlation problems, since a mis-match of large $\delta^{13}C$ variations in the Miocene ($\geq$ 0.5 ‰) could produce artificial basin-to-basin differences. However, by integrating the $\delta^{18}O$ stratigraphy with magnetostratigraphy and biostratigraphy, we believe that interbasinal correlations have a resolution of much better than 0.5 m.y. [Miller et al., 1991b; Wright and Miller, 1991].

CARBON ISOTOPES

Synoptic $\delta^{13}C$ variations in excess of 0.5 ‰ occurred in all oceans during the late Miocene, reflecting changes in the global oceanic carbon reservoir (Figure 2). These global $\delta^{13}C$ fluctuations resulted from variations in the input of riverine bicarbonate $\delta^{13}C$ values and/or burial ratio of organic carbon to calcium carbonate [Miller and Fairbanks, 1985; Vincent and Berger, 1985; Shackleton, 1987] independent of deepwater circulation induced $\delta^{13}C$ differences. The effects of deepwater circulation patterns were superimposed on global $\delta^{13}C$ changes. Therefore, site-to-site $\delta^{13}C$ differences should reflect deepwater circulation patterns.

A comparison of North Atlantic (Sites 563 and 608) and Pacific (Site 289) $\delta^{13}C$ records provides a first-order look at late Miocene deepwater circulation patterns. Late Miocene $\delta^{13}C$ values in the North Atlantic were higher than those in the Pacific for all but a brief period (Figure 2). During the early late Miocene (10.4-7.5 Ma), the North Atlantic-Pacific $\delta^{13}C$ differences averaged 0.5 to 0.8 ‰, equivalent to one half to two thirds of the modern difference. At 8.6 Ma, North Atlantic and Pacific $\delta^{13}C$ values were similar, but the difference soon increased to 0.5 ‰. In the latest Miocene (7.5-5.3 Ma), these interbasinal $\delta^{13}C$ differences increased to the modern value of 1.0 ‰. There is some speculation that the eastern basins of the North Atlantic were isolated from the flux of NCW during the early Miocene [Miller et al., 1986]. However, the upper Miocene $\delta^{13}C$ records from Sites 563 and 608 are similar (Table 2).

During the late Miocene, $\delta^{13}C$ values from the Southern Ocean (Sites 360 and 704) varied between the high North Atlantic values and the low Pacific values, reflecting changing inputs from each ocean. At the beginning of the late Miocene, Sites 360 and 704 recorded different $\delta^{13}C$ values (Figure 2). From 10.4 to 10.0 Ma, $\delta^{13}C$ values at Site 704 were as high as those in the North Atlantic (Figure 2a), while $\delta^{13}C$ values at Site 360 were approximately 0.25 ‰ less (Figure 2b). Between 10.0 and 9.3 Ma, both sites recorded similar $\delta^{13}C$ values that varied from 0.2 to 0.5 ‰ less than values in the North Atlantic but were always higher than those at Pacific Site 289 (Figure 2).

At 9.2 Ma, an abrupt $\delta^{13}C$ decrease of 0.75 ‰ occurred at Site 704, attaining values equal to Pacific values (Figure 2a). This abrupt decrease is not represented at Site 360 because of a coring gap, but low $\delta^{13}C$ values similar to those at Site 704 were recorded at Site 360 by 9.0 Ma (Figure 2b). Carbon isotope values at Sites 360 and 704 appear to have been intermediate between those in the North Atlantic and Pacific from 8.9 to 8.6 Ma. Differences in $\delta^{13}C$ values among North Atlantic, Pacific, and Southern oceans decreased and ultimately converged at 8.6 Ma (Figures 2a and 2b). From 8.6 to 8.0 Ma, $\delta^{13}C$ values from Sites 360 and 704 were similar to those in the North Atlantic. However, the difference in $\delta^{13}C$ values between the North Atlantic and Pacific remained low ($\leq$0.5 ‰, Figure 2).

Sites 360 and 704 again recorded different $\delta^{13}C$ values from 8.0 to 6.4 Ma (Figure 2). The $\delta^{13}C$ character at Site 360 was intermediate between the North Atlantic and the Pacific during this interval. Site 704 recorded $\delta^{13}C$ values as high as those in the North Atlantic until 6.4 Ma, when $\delta^{13}C$ values shifted to values intermediate between the North Atlantic and Pacific, like those at Site 360. At 7.0 Ma, site-to-site $\delta^{13}C$ differences and absolute values from the North Atlantic, Pacific, and Southern oceans attained a character similar to the modern and Pleistocene end-member signals reported by Oppo and Fairbanks [1987]: $\delta^{13}C$ values were approximately 1.0 ‰ in the North Atlantic, 0.0 ‰ in the Pacific, and 0.5 ‰ in the Southern Ocean (Figure 2).

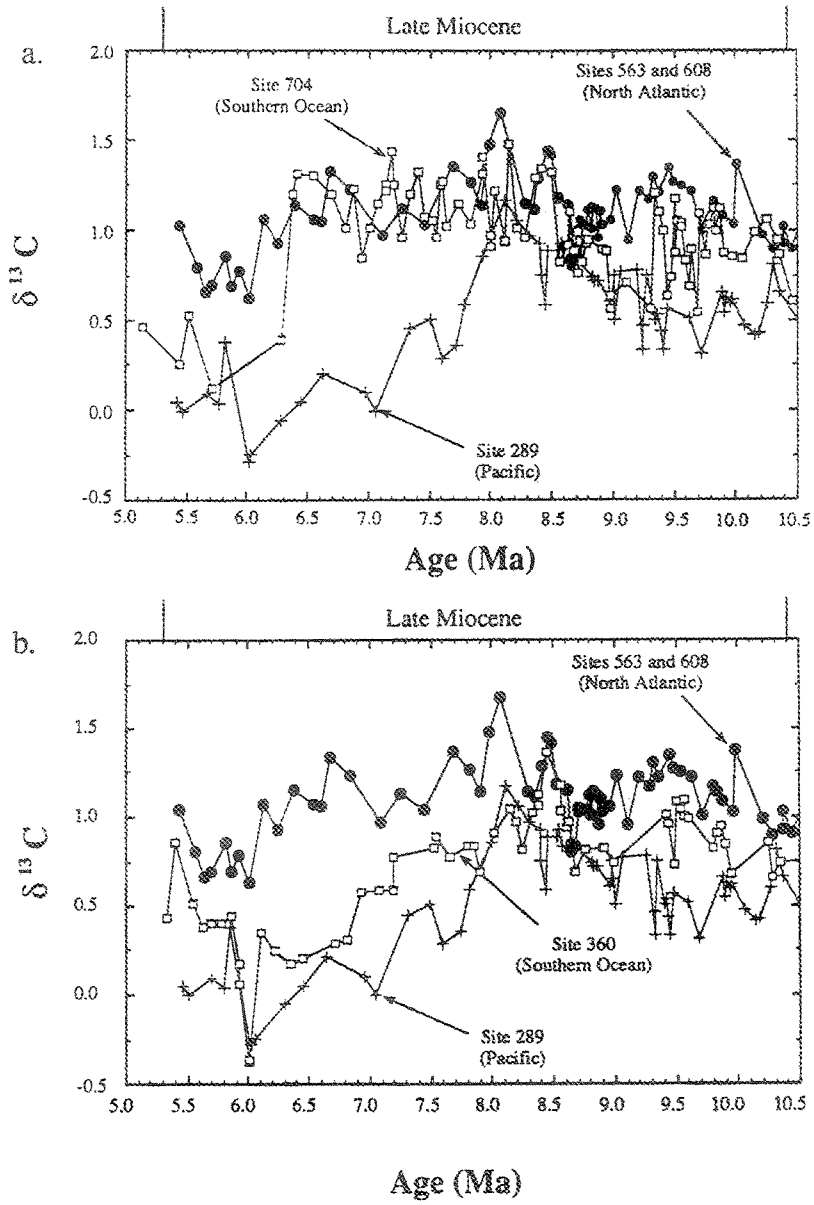

Fig. 2. Late Miocene $\delta^{13}C$ comparisons between North Atlantic Sites 563 and 608 (solid circles), Southern Ocean Sites 704 (Figure 2a) and 360 (Figure 2b) (squares), and Pacific Ocean Site 289 (pluses).

DISCUSSION

Interpretation of Deepwater Circulation from Southern Ocean $\delta^{13}C$ Values

We followed the strategy of Oppo and Fairbanks [1987] in recognizing the value of the Southern Ocean as a monitor of deepwater circulation changes. The percentage of NCW versus POW within the Southern Ocean can be calculated by comparing the Southern Ocean $\delta^{13}C$ values to the NCW (North Atlantic Sites 563 and 608) and POW (Site 289) end-members. We removed global $\delta^{13}C$ variations by subtracting the Pacific record from the Southern Ocean and North Atlantic records, leaving the residual circulation-induced $\delta^{13}C$ differences (Figure 3a). The percentage of NCW versus POW at the Southern Ocean sites (Figure 3b) was calculated using the following equation:

$$\%NCW = \frac{\delta^{13}C_{SO} - \delta^{13}C_{Pac}}{\delta^{13}C_{NA} - \delta^{13}C_{Pac}} \times 100$$

where the subscripts SO, Pac, and NA refer to the Southern, Pacific, and North Atlantic oceans, respectively. The sensitivity of the Southern Ocean to changes in the relative

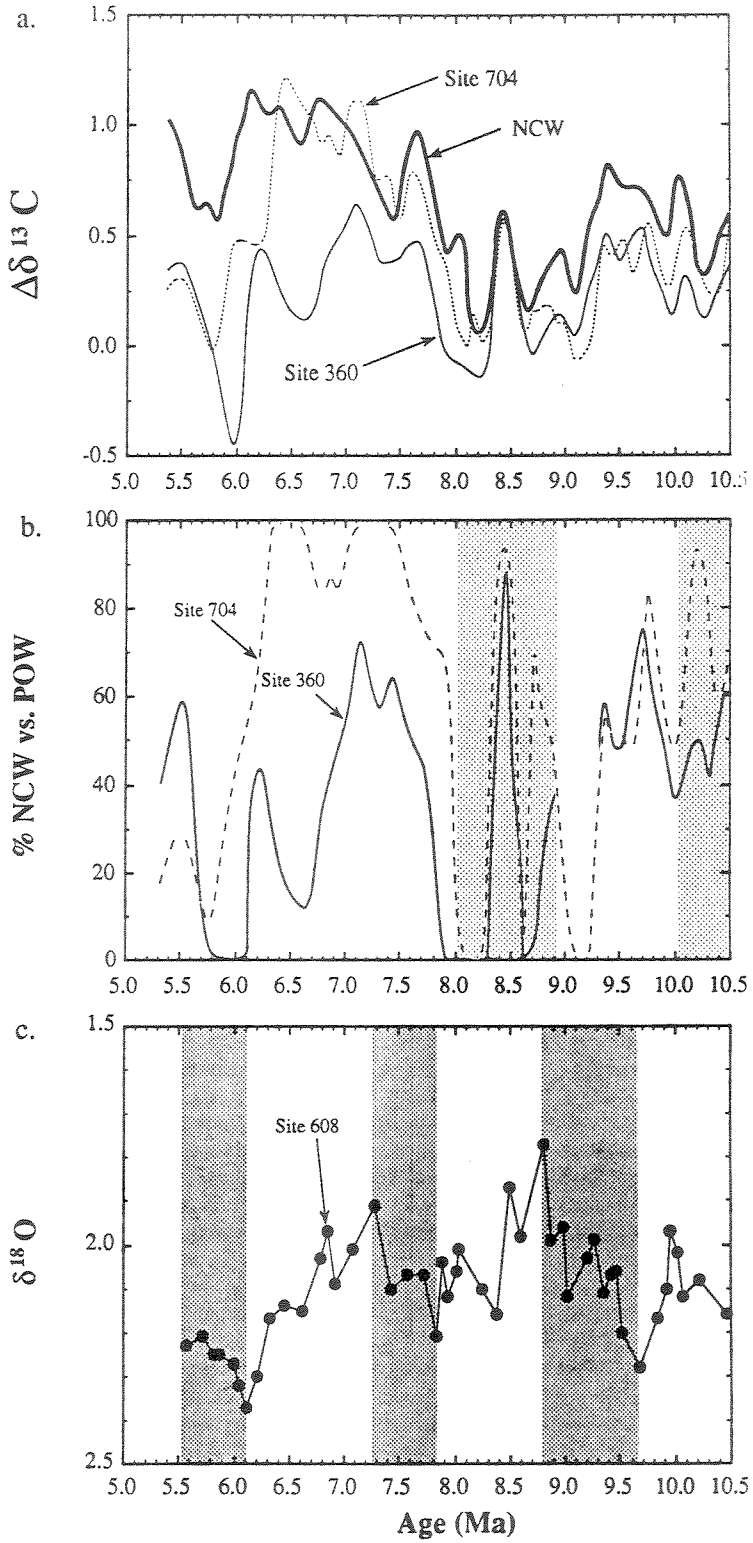

Fig. 3. (a) Atlantic-Pacific and Southern Ocean-Pacific differences in $\delta^{13}C$ values during the late Miocene. These differences were calculated by interpolating each record to 50-kyr. intervals, smoothing with a 250 kyr. Gaussian convolution filter, and subtracting the POW $\delta^{13}C$ records from the North Atlantic (thick line) and Southern Ocean Sites 360 (thin line) and 704 (thin dotted line). (b) The percentage of NCW versus POW reaching Southern Ocean Sites 360 (solid line) and 704 (dotted line). Shaded regions indicate intervals of uncertain flux determinations because the $\delta^{13}C$ difference between the NCW and POW end-members was low. (c) The benthic foraminiferal $\delta^{18}O$ record from Site 608. The shaded areas indicate intervals of decreasing $\delta^{18}O$ values which are interpreted as "interglacials" after Miller et al. [1991b] and Wright and Miller [1991].

flux of end-members is reduced when the $\delta^{13}C$ difference between the NCW and POW end-members is low. As a result of low Atlantic-Pacific differences in $\delta^{13}C$ values (<0.5 ‰), estimates of the NCW flux are difficult to quantify from 10.4 to 10.0 Ma and 8.9 to 8.0 Ma (Figure 3b), although the first-order circulation patterns are clear.

During the early late Miocene (9.8-9.3 Ma), $\delta^{13}C$ values in the Southern Ocean recorded a high contribution from NCW, similar to fluxes in the late Pleistocene (Figures 2 and 3). The percentage of NCW at Site 704 varied from 50% to 90%, while Site 360 recorded NCW contributions between 40% and 80% (Figure 3b). (Higher-frequency changes in NCW flux may be indicated by high $\delta^{13}C$ values at 9.8, 9.5, and 9.3 Ma and low values at 9.6 and 9.4 Ma (Figure 2).) The higher percentage of NCW at Site 704 versus Site 360 is reversed from the present, when NCW contribution to Sites 360 and 704 is 70% and 60%, respectively (Table 1 and Figure 3b). As discussed below, we attribute the difference between the late Miocene and modern $\delta^{13}C$ patterns at Sites 360 (~3000 m paleodepth) and 704 (~2400 m paleodepth) to depth differences between the sites.

The interval between 9.2 and 8.0 Ma is characterized by low interbasinal differences in $\delta^{13}C$ values. At 9.2 Ma, the $\delta^{13}C$ differences between the Pacific and Southern oceans decreased, signaling a sharp reduction in the contribution of NCW to the Southern Ocean (Figure 3). From 9.2 to 8.6 Ma, the difference between the North Atlantic, Pacific, and Southern oceans continued to decrease until the $\delta^{13}C$ values in all three oceans were the same by 8.6 Ma (Figure 2). During this interval of decreased NCW flux, the mixing zone boundary between NCW and SCW moved to the north of Sites 360 and 704 at 9.2 Ma and to the north of Sites 563 and 608 by 8.6 Ma (Figure 2). We interpret the convergence of $\delta^{13}C$ values at 8.6 Ma as a shutdown in NCW production, which allowed SCW to fill most of the deep North Atlantic. The $\delta^{13}C$ values of the Southern Ocean and therefore those in the North Atlantic were similar to POW, which was the dominant influence on the Southern Ocean at that time. With the exception of a brief episode at 8.5 Ma, interbasinal $\delta^{13}C$ differences remained low until 8.0 Ma. The $\delta^{13}C$ values at 8.5 Ma may indicate that there may have been a pulse of NCW production at that time; however, in general, there was little to no NCW flux between 8.9 and 8.0 Ma (Figure 3b).

Sites 360 and 704 recorded different $\delta^{13}C$ values from 8.0 to 6.4 Ma. The $\delta^{13}C$ differences were reversed relative to the modern (see above) from 8.0 to 6.4 Ma, with Site 704 having a higher $\delta^{13}C$ value and apparently recording 100% NCW, while Site 360 was bathed by 10-70% NCW. Today, steep gradients within the NCW and SCW mixing zone clearly demonstrate that small changes in the frontal position can produce large effects in the distribution of $\delta^{13}C$ values (Figure 1) [Oppo and Fairbanks, 1987; Oppo et al., 1990]. The 500 m difference in depth between Sites 360 and 704 must account for the $\delta^{13}C$ differences. Site 360, being at a greater paleodepth (~3000 m), more accurately recorded SCW from 8.0 to 6.4 Ma, while water at Site 704 (~2500 m) was influenced by a high $\delta^{13}C$ intermediate water mass or by a larger percentage of NCW [Charles and Fairbanks, 1990]. Using Site 360 as the more faithful monitor of deepwater fluxes (Figure 3b), we suggest that the contribution of NCW to the Southern Ocean was (1) high from 9.8 to 9.3 Ma, 7.8 to 7.0 Ma, and after 5.8 Ma; (2) low from 9.2 to 8.9 Ma, 7.0 to 6.5 Ma, and 6.1 to 5.8 Ma; and (3) indeterminate from 10.4 to 10.0 Ma and 8.9 to 8.0 Ma.

Deepwater Circulation and Climate

Several studies have related NCW production to late Pleistocene climate changes [Broecker et al, 1990; Birchfield and Broecker, 1990; Charles and Fairbanks, manuscript in preparation]. Late Miocene climate changes also appear to be linked to NCW production, albeit on different times scales. Miller et al. [1991] and Wright and Miller [1991] interpreted two large $\delta^{18}O$ increases with maxima at 9.7 and 8.4 Ma as ice volume increases (Figure 3b). An additional $\delta^{18}O$ maximum occurred at 6.1 Ma, but it was not formally recognized by Miller et al. [1991] and Wright and Miller [1991] because they lacked corroboration from additional sites. The $\delta^{18}O$ decreases associated with these maxima occurred from 9.7 to 8.8 Ma, 7.8 to 7.2 Ma, and 6.1 to 5.5 Ma and are interpreted as "interglacial" intervals (Figure 3b). The largest NCW fluxes were recorded from 9.8 to 9.3 Ma, 7.8 to 7.0 Ma, and after 5.8 Ma, each of which correlates with an "interglacial" interval (Figure 3). Conversely, intervals of increasing $\delta^{18}O$ values correspond to low or indeterminate NCW production (Figure 3). Therefore, we speculate that changes in the relative production of NCW the late Miocene may have been responsible for the transition from "glacial" to "interglacial" climates. These observations need to be tested with more detailed records (i.e., 10^4-10^5 year resolution).

Sedimentological Changes in the North Atlantic

Variations in the production of NCW should be recorded by sedimentation patterns in the North Atlantic. A detailed study of North Atlantic sedimentation patterns in the late Miocene supports our interpretation of $\delta^{13}C$ patterns. Bohrmann et al. [1990] measured carbonate and biosiliceous accumulation rates in the North Atlantic and Norwegian-Greenland Sea. They interpreted high carbonate and low biosiliceous accumulation rates in the Norwegian Sea from 10.2 to 9.3 Ma, and 8.7 to 8.2 Ma as times of high NCW production. These intervals were separated by an interval of low carbonate and high biosiliceous accumulation resulting from low NCW production. These sedimentation patterns are remarkably consistent with our scenario which suggests that the NCW flux was high from 9.8 to 9.3 Ma, reduced or absent from 9.3 to 8.9 Ma, and indeterminate from 8.9 to 8.0 Ma (Figure 3). A hiatus from 7.8 to 5.9 Ma in the Norwegian Sea and the accumulation of terrigenous sediments on the Erik Ridge from 7.5 to 7.0 Ma was interpreted as initiation of Denmark Straits overflow [Bohrmann et al., 1990]. Again, this is consistent with $\delta^{13}C$ comparisons which suggest that NCW was produced from 7.8 to 7.0 Ma (Figure 3).

North Atlantic-Pacific $\delta^{13}C$ Differences

Carbon isotope studies in late Miocene have focused on the global decease in $\delta^{13}C$ values around 6.2 Ma (the "carbon shift" of Keigwin [1979; 1987] and Bender and Keigwin [1979]). To explain this change in deep ocean $\delta^{13}C$ values,

Bender and Keigwin [1979] considered the effects of changes in (1) the global marine phosphorous balance; (2) the global marine carbon balance with respect to $\delta^{13}C$ or ΣCO_2; (3) the internal cycling of nutrients; (4) the upwelling rate; and (5) the deepwater circulation patterns. Although there was a sharp $\delta^{13}C$ decrease in many records at 6.2 Ma [Keigwin, 1979], the late Miocene "carbon shift" can be viewed as a global decrease from 8 to 6 Ma (Figure 2). Because this decrease occurred over a 2 m.y. interval (10 times the residence time of carbon within the ocean [Broecker and Peng, 1982]), this global decrease in deep ocean $\delta^{13}C$ values must represent a change in the input or output ratio of inorganic to organic carbon [Miller and Fairbanks, 1985].

During the global $\delta^{13}C$ decrease from 8 to 6 Ma, the difference between the Atlantic and the Pacific $\delta^{13}C$ values increased. Prior to 7.5 Ma, these interbasinal $\delta^{13}C$ differences were one half to two thirds of the modern difference. The Atlantic-Pacific $\delta^{13}C$ difference increased to 1.0 ‰ by 7.0 Ma and persisted through the rest of the late Miocene (Figure 2). For this discussion, we will consider three mechanisms which may have changed the $\delta^{13}C$ differences between the North Atlantic and Pacific during the late Miocene: (1) changes in deepwater circulation patterns; (2) increased mean oceanic nutrient concentrations; and (3) decreased preformed nutrients in NCW.

Hypothesis 1: Changing the Deepwater Circulation Patterns

As discussed earlier, lower $\delta^{13}C$ differences between the North Atlantic and Pacific may be attributed to changes in NCW flux. Reduced NCW production or enhanced SCW production would allow more SCW water to fill the North Atlantic, decreasing the $\delta^{13}C$ difference between the deep North Atlantic and the Pacific [Bender and Keigwin, 1979]. Sites 563 and 608 are south of the region of NCW formation and their $\delta^{13}C$ records may have had a large SCW influence. At times of reduced NCW flux, an increased percentage of SCW at Sites 563 and 608 would have reduced the apparent $\delta^{13}C$ difference between the North Atlantic and Pacific oceans. The $\delta^{13}C$ differences between Site 563 in the North Atlantic and Site 289 in the Pacific would be less than if true NCW were measured. This would produce an artificially low $\delta^{13}C$ difference between these basins. We favor this hypothesis as a partial explanation for low $\delta^{13}C$ differences between the North Atlantic and Pacific from 10.4 to 10.0 Ma and 8.9 to 8.0 Ma (Figure 3). However, decreased NCW flux cannot fully account for the low $\delta^{13}C$ differences from 10.4 to 9.3 Ma. In this interval, the Southern Ocean recorded high contributions from NCW, yet the Atlantic-Pacific $\delta^{13}C$ differences were only moderate at 0.5-0.8 ‰ (Figure 3a). In contrast, similar relative contributions of NCW were recorded in the latest Miocene, but the Atlantic-Pacific difference in $\delta^{13}C$ values was ~1.0 ‰ (Figure 3a).

Hypothesis 2: Increased Nutrient Concentrations

Changes in the mean oceanic nutrient levels affect changes in $\delta^{13}C$ differences between basins independent of deepwater circulation patterns [Broecker, 1982]. During the early late Miocene (10.4-7.5 Ma), lower $\delta^{13}C$ differences between the North Atlantic and the Pacific may be ascribed to lower mean oceanic nutrient levels relative to the latest Miocene and today. Two proxies provide an estimate of nutrient distribution within the world's ocean: (1) the difference between phosphate-free warm surface $\delta^{13}C$ values and mean ocean $\delta^{13}C$ values [Broecker, 1982; Shackleton et al., 1983]; and (2) Cd/Ca ratios from benthic foraminifera [Boyle, 1986]. For the late Miocene comparisons, we chose planktonic and benthic foraminiferal $\delta^{13}C$ records from the western equatorial Pacific Site 289 [Savin et al., 1981, 1985] and the planktonic record from subtropical Site 590 [Kennett, 1986]. The benthic $\delta^{13}C$ record from Site 289 provides an approximation of mean deepwater (MDW) $\delta^{13}C$ values [Shackleton et al., 1983]. Surface waters at Site 289 today are not phosphate free [Broecker and Peng, 1982]; however, comparison with values from Site 590 whose surface waters are phosphate free today shows only minor differences between the two planktonic records (Figure 4).

Surface-to-deepwater $\delta^{13}C$ differences were low in the middle and early late Miocene (averaging 1.4 ‰), which is two-thirds of the modern difference (Figure 4b). This difference increased in the late Miocene to near modern values of ~2.0 ‰. The timing of this increase is uncertain. Planktonic values from Site 289 suggest that a $\delta^{13}C$ difference similar to today's was attained by 9.0 Ma, in contrast to values from Site 590, which place the increase between 8.0 and 7.5 Ma (Figure 4b). This discrepancy may result from lower sample resolution at Site 289 between 9.2 and 8.6 Ma.

The correlation of modern oceanic Cd and P is excellent even though the biogeochemical link between these tracers is not known. The ratio at which Cd is incorporated into foraminiferal calcite relative to Ca provides an approximation of the P concentration in the water [Boyle, 1986]. The extent to which Boyle's [1986] relationship between oceanic Cd/Ca ratios and P concentrations can be extrapolated to longer time scales is still in doubt. However, we assume that late Miocene Cd/Ca ratios from the Pacific Ocean reflect mean oceanic nutrient levels. Using Cd/Ca ratios from Site 289, Delaney and Boyle [1987] concluded that: (1) late Miocene Cd/Ca inventories were lower than today and (2) the $\delta^{13}C$ change across the late Miocene "carbon shift" at ca. 6.2 Ma was not accompanied by an equivalent Cd/Ca change. Their conclusions used averages of the Cd/Ca data and assumed that there was no systematic species offset between Cd/Ca ratios of *Uvigerina* spp., *Cibicidoides mundulus*, and *P. wuellerstorfi* [Boyle and Keigwin, 1985]. However, there is some evidence that indicates that Cd/Ca ratios may not be similar among species [McCorkle and Klinkhammer, 1988]. As a result, we interpreted the Cd/Ca ratios from only *P. wuellerstorfi* and found it to be consistent with the observed interbasinal differences in $\delta^{13}C$ values.

Cadmium/calcium ratios in *P. wuellerstorfi* at Site 289 fluctuated about a mean value of 0.12 μmol/mol between 15.0 and 8.0 Ma (Figure 4c). The ratios in this interval were approximately one half to two thirds of the modern Pacific value (0.172 μmol/mol) [Boyle, 1986]. This difference may be explained by lower mean oceanic nutrient levels in the late Miocene relative to today's levels (Figure 4c). If Pacific Cd/Ca ratios in *P. wuellerstorfi* approximated middle and late Miocene nutrient levels, then a Cd/Ca ratio of 0.12 μmol/mol

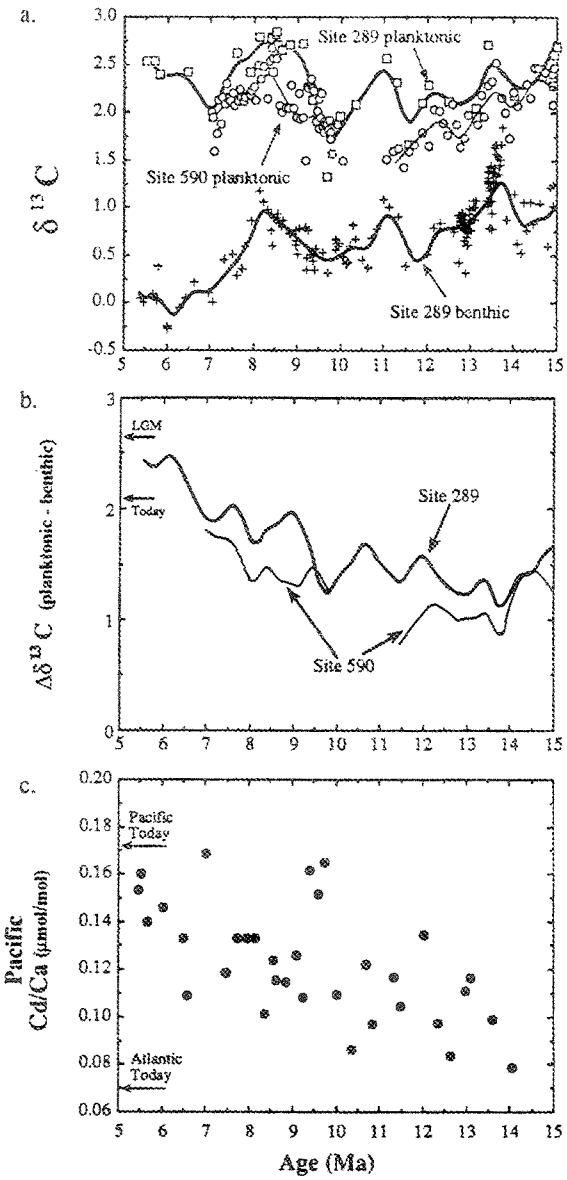

Fig. 4. (a) Middle and late Miocene planktonic (squares) and benthic (pluses) foraminiferal $\delta^{13}C$ records from Site 289 and planktonic foraminiferal record from Site 590 (open circles), (b) planktonic-benthic $\delta^{13}C$ difference (Site 289 benthic record was subtracted from both planktonic records), and (c) *Planulina wuellerstorfi* Cd/Ca ratios from Site 289 [from Delaney and Boyle, 1987 and Delaney, 1990].

implies that the mean oceanic nutrient concentrations were approximately 30% lower than today from 15.0 to 8.0 Ma. The corresponding surface-to-deepwater and NCW to POW differences in $\delta^{13}C$ values would have been 1.4 and 0.7 ‰, respectively (Figures 2 and 4c), similar to that observed. Our middle and early late Miocene nutrient level estimates are in agreement with Delaney's [1990] estimate of 20% lower concentrations.

By 6.0 Ma, Site 289 Cd/Ca ratios increased to 0.16 μmol/mol, approaching the modern Pacific value (Figure 4c). Again, if Site 289 was representative of late Miocene MDW, then a ratio of 0.16 μmol/mol suggests that nutrient levels were 90% of the modern level. The predicted surface-to-deepwater and NCW to POW differences in $\delta^{13}C$ would have been 1.85 and 0.9 ‰, respectively, similar to those observed (Figures 2 and 4b). Thus, both planktonic-benthic foraminiferal $\delta^{13}C$ differences and Cd/Ca ratios suggest that MDW nutrient levels were lower from 10.4 to 7.5 Ma than from 7.5 to 5.3 Ma.

Lower mean oceanic nutrient levels may have contributed to the lower $\delta^{13}C$ differences between the North Atlantic and Pacific in the early late Miocene relative to the latest Miocene. An increase in MDW nutrient levels at 7 Ma would have increased the organic carbon flux or respired CO_2 in the deep reservoir, lowering its $\delta^{13}C$ value [Bender and Keigwin, 1979]. Because NCW is nutrient-depleted, most of the added CO_2 would be stored in the deep Pacific, increasing the contrast in North Atlantic-Pacific $\delta^{13}C$ values [Bender and Keigwin, 1979]. Clearly, the combination of hypotheses one and two can adequately explain the observed in the late Miocene $\delta^{13}C$ patterns in terms of end-member differences and absolute values. Much of the difference in the Atlantic-Pacific $\delta^{13}C$ values can be ascribed to deepwater circulation changes, and they, to a degree, reflect the history of NCW production. However, MDW nutrient changes appear to have modulated the dynamic range of this difference by 20 to 30%.

Hypothesis 3: Increased Preformed Nutrients in Northern Component Water

A third hypothesis concerns regional chemistry changes in the North Atlantic [Mix and Fairbanks, 1985]. Today, the Atlantic-Pacific $\delta^{13}C$ difference is a result of nutrient-depleted, high $\delta^{13}C$ source water feeding NADW. North Atlantic Deep Water production creates a lagoonal circulation pattern in the North Atlantic [Stommel, 1957; Worthington, 1970; Berger, 1970; Gordon and Piola, 1983; Warren, 1983]. Upper layer water (thermocline and surface) is drawn into the northern North Atlantic to replace the sinking water, allowing the processes of evaporation and sinking to continue. Thus, the NCW nutrient and $\delta^{13}C$ characteristics represent those of the sinking surface water and entrained thermocline water which have low nutrient and high $\delta^{13}C$ values [Broecker and Peng, 1982; Gordon and Piola, 1983; Gordon, 1986].

Lower $\delta^{13}C$ differences between the North Atlantic and Pacific in the early late Miocene (10.4-7.5 Ma) could have been a result of higher nutrients in NCW source water relative to the present. Increased nutrient levels and accompanying low $\delta^{13}C$ values in NCW would have decreased the Atlantic-Pacific $\delta^{13}C$ difference relative to today. The $\delta^{13}C$ value of NCW could have been lowered through the transfer of nutrients from the Pacific into the North Atlantic by thermocline and/or surface water. Two possible paths existed for this exchange. The first requires a cross-equatorial transfer via South Atlantic thermocline water [Gordon, 1986]. Alternatively, surface and thermocline water could have been directly injected into the North Atlantic across Panama [Luyendyk et al, 1972; Bender and Keigwin, 1979], because the marine connections across the isthmus did not terminate until 4-3 Ma [Keigwin, 1978; Bender and Keigwin, 1979]. In each case, more nutrients may

have been transferred from the Pacific to the North Atlantic than at present, resulting in lower $\delta^{13}C$ differences between the North Atlantic and Pacific (Figure 2).

The validity of this hypothesis to explain the observed $\delta^{13}C$ patterns cannot be evaluated at present. Although we cannot exclude this hypothesis, we note that the $\delta^{13}C$ patterns can be explained well by a combination of hypotheses 1 and 2.

Evolution of Modern $\delta^{13}C$ Patterns

By 7.0 Ma, the distribution of $\delta^{13}C$ values in the deep and intermediate ocean was similar to the present (Figure 2). Southern Ocean $\delta^{13}C$ values fluctuated between the high North Atlantic values and the low Pacific values (Figure 3). The mean $\delta^{13}C$ value was ~1.0 ‰ in the deep North Atlantic and 0.0 ‰ in the Pacific (Figure 2). Carbon isotope values from Sites 360 and 704 fluctuated about a mean of 0.6 ‰, similar to today. Pacific Outflow Water $\delta^{13}C$ values were always the lowest recorded of any deepwater mass. Both surface-to-deep $\delta^{13}C$ differences and Cd/Ca ratios in the Pacific indicate that nutrient levels were near today's levels by the end of the late Miocene (Figure 4). Additionally, the 1 ‰ difference in Atlantic and Pacific $\delta^{13}C$ values implies that NCW was nutrient-depleted and had high $\delta^{13}C$ values by this time. These patterns are the first record of modern $\delta^{13}C$ differences and indicate that modern deepwater characteristics evolved in the latest Miocene [Bender and Keigwin, 1979] and continued into the Plio-Pleistocene [Oppo and Fairbanks, 1987; Oppo et al., 1990; Raymo et al., 1989; Hodell and Ciesielski, 1990].

We suggest that the evolution of $\delta^{13}C$ patterns in the latest Miocene, which resembled those in the present ocean, resulted partly from an increase in MDW nutrient levels. Changes in the flux of NCW also controlled the $\delta^{13}C$ patterns in the late Miocene, as evidenced by contrasting $\delta^{13}C$ patterns from 9.8 to 9.3 Ma (high NCW flux) with those from 8.9 to 8.0 Ma (low NCW flux). However, deepwater circulation changes cannot fully explain observed $\delta^{13}C$ changes. Late Miocene $\delta^{13}C$ differences documented similar fluxes of NCW during two intervals, from 9.8 to 9.3 Ma and 7.5 to 5.3 Ma. A comparison of these intervals shows that the $\delta^{13}C$ differences between the North Atlantic and Pacific were lower during the interval from 9.8 to 9.3 Ma than during the interval from 7.5 to 5.3 Ma (Figure 3). We attribute this not only to a NCW flux at 7.5 Ma, but also by an increase in MDW nutrient levels, which increased the dynamic range of $\delta^{13}C$ values between the end-members.

CONCLUSIONS

The Southern Ocean recorded high NCW fluxes from 9.8 to 9.3 Ma and 7.5 to 5.3 Ma. There was little NCW contribution to the Southern Ocean from 9.2 to 8.9 Ma. End-member $\delta^{13}C$ differences were low between 8.9 and 8.0 Ma, hindering exact flux estimates. These lower interbasinal $\delta^{13}C$ differences probably reflected lower NCW production from 9.2 to 8.0 Ma and an increase in the percentage of SCW reaching the North Atlantic. A complete shutdown of NCW production at 8.6 Ma is indicated by the convergence of North Atlantic, Pacific, and Southern Ocean $\delta^{13}C$ values.

By 7.0 Ma, modern $\delta^{13}C$ differences developed; North Atlantic values oscillated around 1.0 ‰, and Pacific values were near 0.0 ‰, with Southern Ocean values intermediate between the two end-members. These $\delta^{13}C$ patterns were partially controlled by the flux of NCW. In addition to the high flux of NCW, mean nutrient levels must have increased during the late Miocene to produce the near modern $\delta^{13}C$ patterns by 7 Ma.

We speculate that there was a direct link between NCW production and climate change during the late Miocene. Decreasing $\delta^{18}O$ values, which are interpreted as decreasing ice volume or "interglacial" intervals, occurred during intervals of high NCW production. Conversely, intervals of increasing $\delta^{18}O$ values or "glacial" intervals occurred during intervals of low or indeterminate NCW production.

Acknowledgements. We would like to thank S. Savin, J. Zachos, L. Burckle, and M. Katz for reviews. We would also like to thank C. Charles, D. Oppo, and N. Slowey for helpful discussions. This work was supported by NSF Grants OCE85-21690 and OCE88-11834 to K. Miller and OCE88-19438 to R. Fairbanks. This is Lamont-Doherty Geological Observatory contribution 4745.

REFERENCES

Andrews, J.E. et al., *Initial Reports of the Deep Sea Drilling Project, vol.* 30, U.S. Government Printing Office, Washington, D.C., 1975.

Barker, P.F., and J. Burrell, The opening of Drake Passage, *Mar. Geol., 25*, 15-34, 1977.

Belanger, P.E., W.B. Curry, and R.K. Matthews, Core-top evaluation of benthic foraminiferal isotopic ratios for paleo-oceanographic interpretations, *Palaeogeogr. Palaeoclimatol. Palaeocol., 33*, 205-220, 1981.

Bender, M.L., and L.D. Keigwin, Speculations about the upper Miocene change in abyssal Pacific dissolved bicarbonate $\delta^{13}C$, *Earth Planet. Sci. Lett., 45*, 383-393, 1979.

Berger, W.H., Biogenous deep-sea sediments: Fractionation by deep-sea circulation, *Geol. Soc. Am. Bull., 81*, 1385-1402, 1970.

Berger, W.H., and E.L. Winterer, Plate stratigraphy and the fluctuation carbonate line, in Pelagic Sediments on Land Under the Sea, edited by K.J. Hsu and H. C. Jenkins, *Spec. Publ. Int. Assoc. Sedimentol., 1*, 11-48, 1974.

Berggren, W.A., and J.A. Van Couvering, The late Neogene: Biostratigraphy, geochronology and paleoclimatology of the last 15 million years in marine and continental sequences, *Palaeogeogr. Palaeoclimatol. Palaeocol., 16*, 1-216, 1974.

Berggren, W.A., D.V. Kent, and J.A. Van Couvering, Neogene geochronology and chronostratigraphy, in *The Chronology of the Geological Record*, edited by N.J. Snelling, pp. 211-260, Geological Society, London, 1985.

Birchfield, G.E., and W.S. Broecker, A salt oscillator in the glacial Atlantic: 2. A "Scale Analysis" model, *Paleoceanography, 5*, 835-843, 1990.

Blanc, P.-L., and J.C. Duplessy, The deepwater circulation during the Neogene and the impact of the Messinian salinity crisis, *Deep Sea Res., 29A*, 1391-1414, 1982.

Bohrmann, G., R. Henrich, and J. Thiede, Miocene to Quaternary paleoceanography in the northern North Atlantic: Variability in carbonate and biogenic opal accumulation, in

Geologic History of the Polar Oceans: Arctic Versus Antarctic, edited by U. Bleil, pp. 647-675, Kluwer Academic Publishers, Boston, Mass., 1990.

Bolli, H. et al., *Initial Reports of the Deep Sea Drilling Project, vol.* 40, U.S. Government Printing Office, Washington, D.C., 1978.

Bougault, H. et al., *Initial Reports of the Deep Sea Drilling Project, vol.* 85, U.S. Government Printing Office, Washington, D.C., 1985.

Boyle, E.A., Paired Cd and carbon isotope data in benthic foraminifera: implication for changes in ocean phosphorous, ocean circulation and atmospheric carbon dioxide, *Geochim. Cosmochim. Acta, 50*, 256-276, 1986.

Boyle, E.A., The role of vertical chemical fractionation in controlling late Quaternary atmospheric carbon dioxide, *J. Geophys. Res., 93*, 15,701-15,714, 1989.

Boyle, E.A., and L.D. Keigwin, Deep circulation of the North Atlantic over the last 200,000 years, geochemical evidence, *Science, 218*, 784-787, 1982.

Boyle, E.A., and L.D. Keigwin, Comparison of Atlantic and Pacific paleochemical records for the last 215,000 years: Changes in deep ocean circulation and chemical inventories, *Earth Planet. Sci. Lett., 76*, 135-150, 1985.

Boyle, E.A., and L.D. Keigwin, North Atlantic thermohaline circulation during the past 20,000 years linked to high-latitude surface temperature, *Nature, 330*, 35-40, 1987.

Broecker, W.S., A revised estimate for the radiocarbon age of North Atlantic Deep Water, *J. Geophys. Res., 84*, 3218-3226, 1979.

Broecker, W.S., Glacial to interglacial changes in ocean chemistry, *Prog. Oceanogr., 11*, 151-197, 1982.

Broecker, W.S., and G.H. Denton, The role of ocean-atmosphere reorganizations in glacial cycles, *Geochi. Cosmochim. Acta, 53*, 2465-2501, 1989.

Broecker, W.S., and T.-H. Peng, *Tracers in the Sea*, 690 pp., Eldigio, Palisades, N.Y., 1982.

Broecker, W.S., G. Bond, M. Klaus, G. Bonanai, and W. Wolfli, A salt oscillator in the glacial Atlantic?, 1, The concept, *Paleoceanography, 5*, 469-478, 1990.

Charles, C.D., and R.G. Fairbanks, Glacial to interglacial changes in the isotopic gradients of Southern Ocean surface water, in *Geologic History of the Polar Oceans: Arctic Versus Antarctic*, edited by U. Bleil, pp. 519-538, Kluwer Academic Publishers, Boston, Mass., 1990.

Ciesielski, P.F. et al., *Proceedings of the Ocean Drilling Program, Initial Reports, vol.* 114, Ocean Drilling Program, College Station, Tex., 1988.

Clement, B., and F. Robinson, The magnetostratigraphy of Leg 94 sediments, *Initial Rep. Deep Sea Drill. Proj., 94*, 635-650, 1986.

Curry, W.B., and G.P. Lohmann, Carbon isotopic changes in benthic foraminifera from the western South Atlantic: Reconstruction of glacial abyssal circulation patterns, *Quat. Res., 18*, 218-235, 1982.

Delaney M.L., Miocene benthic foraminiferal Cd/Ca records: South Atlantic and western equatorial Pacific, *Paleoceanography, 5*, 743-760, 1990.

Delaney M.L., and E.A. Boyle, Cd/Ca in late Miocene benthic foraminifera and changes in the global organic carbon budget, *Nature, 330*, 156-159, 1987.

Delmas, R.J., J.M. Ascencio, and M. Legrand, Polar ice evidence that atmospheric CO_2 20,000 BP was 50% of present, *Nature, 284*, 155-157, 1980.

Duplessy, J.C., N.J. Shackleton, R.G. Fairbanks, L. Labeyrie, D. Oppo, and N. Kallel, Deepwater source variations during the last climatic cycle and their impact on the global deepwater circulation, *Paleoceanography, 3*, 343-360, 1988.

Georgi, D.T, On the relationship between the large-scale property variations fine structure in the Circumpolar Deep Water, *J. Geophys. Res., 86*, 6556-6566, 1981.

Gordon, A.L., Interocean exchange of thermocline water, *J. Geophys. Res., 91*, 5037-5046, 1986.

Gordon, A.L. and A.R. Piola, Atlantic Ocean upper layer salinity budget, *J. Phys. Oceanogr., 13*, 1293-1300, 1983.

Graham, D.W., B.H. Corliss, M.L. Bender, and L.D. Keigwin, Carbon and oxygen isotopic disequilibria of Recent benthic foraminifera, *Mar. Micropaleontol., 6*, 483-497, 1981.

Hailwood, E.A., and B.M. Clement, Magnetostratigraphy of ODP Sites 703 and 704, Meteor Rise, southeastern South Atlantic, *Proc. Ocean Drill. Program, Sci. Results, 114*, in press, 1991.

Hamilton, W., Tectonics of the Indonesian region, *U.S. Geol. Surv. Prof. Pap., 1078*, 345 pp., 1979.

Hodell, D.A., and P.F. Ciesielski, Southern ocean response to the onset of northern hemisphere glaciation at 2.4 Ma, in *Geologic History of the Polar Oceans: Arctic Versus Antarctic*, edited by U. Bleil, pp. 707-728, Kluwer Academic Publishers, Boston, Mass., 1990.

Jenkins, D.G., Neogene planktonic foraminifers from DSDP Leg 40 Sites 360 and 362 in the southeastern Atlantic, *Initial Rep. Deep Sea Drill. Proj., 40*, 723-740, 1978.

Keigwin, L.D., Pliocene closing of the Isthmus of Panama, based on biostratigraphic evidence from nearby Pacific Ocean and Caribbean Sea cores, *Geology, 6*, 630-634, 1978.

Keigwin, L.D., Late Cenozoic stable isotope stratigraphy and paleoceanography of DSDP sites from the east equatorial and central North Pacific Ocean, *Earth Planet. Sci. Lett., 45*, 361-382, 1979.

Keigwin, L.D., Toward a high-resolution chronology for latest Miocene paleoceanographic events, *Paleoceanography, 2*, 639-660, 1987.

Kennett, J.P., Miocene to early Pliocene oxygen and carbon isotope stratigraphy in the southwest Pacific, Deep Sea Drilling Project Leg 90, *Initial Repts. Deep Sea Drill. Proj., 90*, 1383-1411, 1986.

Kroopnick, P., The distribution of ^{13}C of ΣCO_2 in the world oceans, *Deep Sea Res.*, 32, 57-84, 1985.

Luyendyk, B.P., D. Forsyth, and J.D. Phillips, Experimental approach to the paleocirculation of the oceanic surface waters, *Geol. Soc. Am. Bull., 83*, 2649-2664, 1972.

Luyendyk, B.P., A. Shor, and J.R. Cann, General implications of the Leg 49 drilling program for North Atlantic Ocean geology, *Initial Rep. Deep Sea Drill. Proj., 49*, 825-840, 1979.

Mantyla, A.W., and J.L. Reid, Abyssal characteristics of the world ocean waters, *Deep Sea Res., 8A*, 805-833, 1983.

McCorkle, D.C., and G.P. Klinkhammer, An estimate of the pore water $Cd/\delta^{13}C$ relationship, *Eos, 69*, p. 1119, 1988.

Miller, K.G., and R.G. Fairbanks, Oligocene to Miocene carbon isotope cycles and abyssal circulation changes, in

The Carbon Cycle and Atmospheric CO_2: Natural Variations Archean to Present, Geophys. Monogr. Ser., vol. 32, edited by E. Sundquist and W.S. Broecker, pp. 469-486, AGU, Washington, D.C., 1985.

Miller, K., and D.V. Kent, Testing Cenozoic eustatic changes: The critical role of stratigraphic resolution, *Spec. Publ. Cushman Found. Foraminiferal Res., 24*, 51-56, 1987.

Miller, K.G., and B.E. Tucholke, Development of Cenozoic abyssal circulation south of the Greenland-Scotland Ridge, in *Structure and Development of the Greenland-Scotland Ridge*, edited by M.H.P. Bott et al., pp. 549-589, Plenum, New York, 1983.

Miller, K.G., M.-P. Aubrey, M.J. Khan, A.J. Melillo, D.V. Kent, and W.A. Berggren, Oligocene-Miocene biostratigraphy, magnetostratigraphy and isotopic stratigraphy of the western North Atlantic, *Geology, 13*, 257-261, 1985.

Miller, K.G., R.G. Fairbanks, and E. Thomas, Benthic foraminiferal carbon isotopic records and the development of abyssal circulation in the eastern North Atlantic, *Initial Rep. Deep Sea Drill. Proj., 94*, 981-996, 1986.

Miller, K.G., J.D. Wright, and A.N. Brower, Oligocene to Miocene stable isotope stratigraphy and planktonic foraminifer biostratigraphy of the Sierra Leone Rise (DSDP Site 366 and ODP Site 667), *Proc. Ocean Drill. Program, Sci. Results*, 108, 279-294, 1989.

Miller, K.G., M.D. Feigenson, J.D. Wright, and B.M. Clement, Miocene isotope reference section, Deep Sea Drilling Project Site 608: An evaluation of isotope and biostratigraphic resolution, *Paleoceanography*, in press, 1991a.

Miller, K.G., J.D. Wright, and R.G. Fairbanks, Unlocking the Icehouse: Oligocene-Miocene oxygen isotope, eustasy, and margin erosion, *J. Geophys. Res.*, in press, 1991b.

Mix, A.C., and R.G. Fairbanks, North Atlantic surface-ocean control of Pleistocene deep-ocean circulation, *Earth Planet. Sci. Lett., 76*, 231-243, 1985.

Neftel, A., H. Oeschger, H. Schwander, B. Stauffer, and R. Zumbrunn, Ice core sample measurements give atmospheric CO_2 content during the past 40,000 yr, *Nature, 295*, 220-223, 1982.

Oeschgar, H., J. Beer, U. Siegenthaler, B. Stauffer, W. Dansgaard, and C.C. Langway, Late glacial climate history from ice cores, in *Climate Processes and Climate Sensitivity, Geophys. Monogr. Ser.*, vol. 29, edited by J. Hansen and T. Takahashi, pp. 299-306, AGU, Washington, D.C., 1983.

Oppo, D.W., and R.G. Fairbanks, Variability in the deep and intermediate water circulation of the Atlantic Ocean during the past 25,000 years: Northern hemisphere modulation of the Southern Ocean, *Earth Planet. Sci. Lett., 86*, 1-15, 1987.

Oppo, D.W., R.G. Fairbanks, and A.L. Gordon, Late Pleistocene Southern Ocean $\delta^{13}C$ variability, *Paleoceanography, 5*, 43-54, 1990.

Raymo, M.E., W.F. Ruddiman, J. Backman, B.M. Clement, and D.G. Martinson, Late Pliocene variation in northern hemisphere ice sheets and North Atlantic Deep Water circulation, *Paleoceanography, 4*, 413-446, 1989.

Rogl, F., and F. F. Steininger, Neogene Paratethys, Mediterranean and Indo-Pacific Seaways. Implications for the paleobiogeography of marine and terrestrial biotas, in *Fossils and Climate*, edited by P. Brenchley, 171-200, John Wiley, New York, 1984.

Ruddiman, W.F. et al., *Initial Reports Deep Sea Drilling Project, vol. 94*, U.S. Government Printing Office, Washington, D.C., 1987.

Savin, S.M., G. Keller, R.G. Douglas, J.S. Killingley, L. Shaughnessy, M.A. Sommer, E. Vincent, and F. Woodruff, Miocene benthic foraminiferal isotope records: A synthesis, *Mar. Micropaleontol., 6*, 423-450, 1981.

Savin, S.M. et al., The evolution of Miocene surface and near-surface Mar. temperatures: Oxygen isotopic evidence, in The Miocene Ocean: Paleoceanography and Biogeography, edited by J.P. Kennett ,*Geol. Soc. Am. Mem. 163*, 49-82, 1985.

Schnitker, D., North Atlantic oceanography as possible cause of Antarctic glaciation and eutrophication, *Nature, 284*, 615-616, 1980.

Sclater, J.G., R.N. Anderson, and N.L. Bell, Elevation of ridges and evolution of the central eastern Pacific, *J. Geophys. Res., 76*, 7888-7915, 1971.

Shackleton, N.J., The carbon isotope record of the Cenozoic: History of organic carbon burial and of oxygen in the ocean and atmosphere, in *Marine Petroleum Source Rocks*, edited by H. Brooks and A.J. Fleet, pp. 423-434, Oxford Blackwell Scientific, London, 1987.

Shackleton, N.J., and N.D. Opdyke, Oxygen isotope and paleomagnetic stratigraphy of equatorial Pacific core V28-238: Oxygen isotope temperatures and ice volumes on a 10^5 year and 10^6 year scale, *Quat. Res., 3*, 39-55, 1973.

Shackleton, N.J., M.A. Hall, J. Line, and C. Chuxi, Carbon isotope data in core V19-30 confirm reduced carbon dioxide in the ice age atmosphere, *Nature, 306*, 319-322, 1983.

Siegenthaler, U., M. Heimann, and H. Oeschger, ^{14}C variations caused by changes in the global carbon cycle, *Radiocarbon, 22*, 177-191, 1980.

Srinivasan, M.S., and J.P. Kennett, Neogene planktonic foraminiferal biostratigraphy and evolution: equatorial to subantarctic, South Pacific, *Mar. Micropaleontol., 6*, 499-533, 1981.

Stauffer, B., A. Neftel, H. Oeschger, and H. Schwander, CO_2 concentration in air extracted from Greenland ice samples, in *Greenland Ice Core: Geophysics, Geochemistry, and the Environment, Geophys. Monogr. Ser.*, vol. 33, edited by C.C. Langway et al., pp. 85-89, AGU, Washington, D.C., 1985.

Stommel, H., A survey of ocean current theory, *Deep Sea Res., 4*, 149-184, 1957.

Thiede, J., and O. Eldholm, Speculations about the paleodepth of the Greenland-Scotland Ridge during late Mesozoic and Cenozoic times, in *Structure and Development of the Greenland-Scotland Ridge*, edited by M.H.P. Bott et al., pp. 445-456, Plenum, New York, 1983.

Vincent, E., and W. H. Berger, Carbon dioxide and polar cooling in the Miocene: The Monterey hypothesis, in *The Carbon Cycle and Atmospheric CO_2: Natural Variations Archean to Present. Geophys. Monogr. Ser.*, vol. 32, edited by E. Sundquist and W.S. Broecker, pp. 455-468, AGU, Washington, D.C., 1985.

Warren, B.A., Why is no deep water formed in the North Pacific?, *J. Mar. Res., 41*, 327-347, 1983.

Weissel, J.K., D.E. Hayes, and E.M. Herron, Plate tectonics

synthesis: The displacements between Australia, New Zealand, and Antarctica since the Late Cretaceous, *Mar. Geol., 25*, 231-277, 1977.

Woodruff, F., and S.M. Savin, Miocene deepwater oceanography, *Paleoceanography, 4*, 87-140, 1989.

Woodruff, F., S.M. Savin, and R.G. Douglas, Miocene stable isotope record: A detailed deep Pacific Ocean study and its paleoclimatic implications, *Science, 212*, 665-668, 1981.

Worthington, L.V., The Norwegian Sea as a mediterranean basin, *Deep Sea Res., 17*, 77-84, 1970.

Wright, J.D., and K.G. Miller, Miocene stable isotope stratigraphy, Site 747, Kerguelen Plateau. *Proc. Ocean Drill. Program, Sci. Results, vol.* 120, in press, 1991.

R.G. Fairbanks and J.D. Wright, Lamont-Doherty Geological Observatory, Palisades, New York 10964.

K.G. Miller, Department of Geological Sciences, Rutgers University, New Brunswick, New Jersey 08903, and Lamont-Doherty Geological Observatory, Palisades, New York 10964.

(Received May 3, 1990;
revised November 6, 1990;
accepted November 8, 1990.)